Random Walker with Fuzzy Initialization Applied to Segment Masses in Mammography Images

Filipe R. Cordeiro and Kallebe F. P. Bezerra
Department of Statistics and Informatics - DEINFO, Federal Rural University of Pernambuco, Brazil
Email: filipe.rolim@ufrpe.br, kallebefelipe@gmail.com

***Abstract*—Segmentation of masses in mammography images is an important task in early detection of breast cancer. Although the quality of segmentation is crucial to avoid misdiagnosis, the segmentation process is a challenging task even for specialists, due to the presence of ill-defined edges and low contrast images. In this work, we propose an improvement on Random Walker algorithm to segment masses, by applying a fuzzy approach in the initialization stage. We evaluated the new approach compared with classical Random Walker, using 57 images of Mini-MIAS database. The segmented images were compared with ground truth, using the metrics of sensitivity, specificity, balanced accuracy, Jaccard index and dice. Results showed that the proposed method obtained better segmentation results when compared with classical Random Walker, requiring lower user interaction.**

***Keywords*-mammography; masses; random walker, fuzzy;**

I. Introduction

Breast cancer has become an increasing problem for women worldwide: according to the World Health Organization (WHO), it is the most common type of cancer in women, with increasing mortality, both for developed and underdevelopment countries, becoming one of the most fatal forms of cancer [1].

Early detection has a substantial impact on the successful treatment of cancer, once medical treatment becomes harder in late stages. One of the most effective methods for breast cancer analysis is digital mammography [2]. However, mammography visual understanding and analysis can be a hard task even to a specialist, once such a procedure can be affected by image quality aspects, radiologist experience, and tumor shape.

After the beginning of breast cancer, the period until tumors become palpable, i.e. reaching a diameter around 1cm, is about ten years [3]. During this time, breast imaging is essential, both for early detection and tumor monitoring. Correct evaluation of the tumor size takes an important role in the planning of the breast cancer treatment, avoiding mutilating surgeries, such as mastectomy [4]. Nevertheless, these methods depend substantially on the professional examiner's experience [5]. Furthermore, image analysis and diagnosis are complex, mainly because of the significant variability of cases. For these reasons, Mammography Computer-Aided Diagnosis (MCAD) has been playing an import role to assist radiologists and other related health professionals in improving the accuracy of their diagnoses. Consequently, traditional techniques in image processing have been applied in the medical field to make diagnosis less susceptible to errors through accurate identification of anatomic anomalies [6][7].

The size of the segmented tumor is a determinant factor in the mammogram diagnosis. It is very related to the malignancy of the tumor, where a difference of just a few centimeters in the maximum diameter can determine whether is necessary to do surgery. However, it can be tough to detect the contour of the tumor accurately depending on several factors, such as tumor shape, density, size, location, and overall image quality. Some challenges in tumor segmentation include low contrast images, intensity levels with considerable variation across different regions, poor illumination, high noise levels, ill-defined contours, and masses not obviously detected [8].

The Random Walker algorithm [9] is a graph based method used for image segmentation, and that has been successfully applied to segmentation of masses in mammography images [10]. In Random Walker, users can obtain feasible results by selecting just a few points from inside and outside the region of interest. However, to achieve higher quality of image segmentation is necessary higher user experience to select the seeds.

In this work, we propose a novel initialization of Random Walker seeds, and we analyze the impact in the segmentation quality. We introduce a labeling step, using a Gaussian fuzzy membership function, which can automatically label background pixels and requires less effort from the user. Results were generated using the Mini-MIAS mammography image database, demonstrating that our approach could reach better results than traditional Random Walker, for the metrics analyzed.

II. Related Work

Region-based segmentation is considered more suitable for mass detection, since regions of the tumor are usually brighter than their surrounding tissues, having almost uniform densities and fuzzy boundaries [8].

Recent studies for tumor segmentation have been successfully applied to region-based techniques for tumor segmentation. Lewis *et. al* [11] employ Watersheds to automatically segment tumor candidate regions, achieving an overall detection rate for mass tumors of 90%. However, the used metric of analysis was based only on tumor location, not on the quality of segmentation.

Eltoukhy and Faye [12] use an adaptive threshold technique, achieving 100% of sensitivity, with an average of 1.87% false positives, when applied to 188 images. However, the value of sensitivity varies depending on the false positive rate, and each work uses a different rate.

Hong proposes a Topographic approach [13] of segmentation, based on the fact that suspicious regions are usually brighter than neighbor regions, with uniform densities. However, for most of the cases, areas of lesion do not have well-defined contours. Due to this fact, seed-based techniques, i.e. techniques in which users label initial seeds, achieve better quality in the final segmentation.

Cordeiro *et. al* [14] apply the classical GrowCut to segment masses in mammograms, obtaining good results regarding the quality of segmentation. Later, Cordeiro *et. al* proposes a Fuzzy approach of GrowCut [15], but the results are only compared with unsupervised methods.

Zen *et. al* [10] use a random-walk based segmentation, obtaining good results of segmentation, but they do not provide quantitative analysis of the experimental results. Although seed-based techniques have shown proper performance for mass segmentation, they require a high level of specialist knowledge about the seed selection problem.

As observed by Raman *et. al* [8], the results obtained with the related state-of-the-art works are significantly different. They are often based on visual subjective opinion with very little quantitative endorsement. Furthermore, most studies describe an accuracy of the techniques based only on the localization of the tumor and not on its shape and contour, very important aspects for accurate diagnoses. Most works discuss the quality of segmentation based on area overlap measure or accuracy. However, a deeper analysis comparing the shape of segmented image and ground-truth is necessary to verify the quality of contour obtained.

III. Random Walker

The Random Walker (RW) segmentation algorithm is a general-purpose interactive segmentation method, originally proposed by Grady [9]. The RW is a graph based method where each pixel is represented as a node, which is connected to its neighbor by the edges. This technique has been used to segment masses in mammograms, finding regions of tumor with high accuracy [10].

The Random Walker approach to segment images is to determine which class a pixel *u* belongs, considering random walks, beginning in *u* and finishing when it arrives at labeled pixel. Next, it is calculated the probability of each label be the first to be reached by a random walk initiated at pixel *u*. The labels with the higher probability of being achieved are set to pixel *u*. The probability of a random walk from pixel *u* until pixel *j* is calculated by Equation 1:

$$p_{uj} = \frac{w_{uj}}{\sum_{k \in N(u)} w_{uk}}, \tag{1}$$

where p_{uj} is the probability of a pixel leave pixel *u* and arrive at pixel *j*, w_{uj} is the weight associated between *u* and *j*, and *N(u)* is the neighbor of *u*. The weight from one pixel to another is calculated by Equation 2:

$$w_{ij} = e^{\frac{-(I_i - I_j)^2}{\sigma^2}}, \tag{2}$$

where I_i and I_j are the intensity values of pixel i and pixel j and σ adjust the value of the the weight. The greater the sigma, the more difficult the diffusion of the segmentation. As the weights represent the differences between pixels values, the walks have higher probabilities of running through uniform regions, avoiding edges. It is known [16] that Random Walker solution also minimizes the energy of Equation 3:

$$\text{Energy} = \frac{1}{2} \sum_{(i,j) \in E} w_{ij} (x_i - x_j)^2, \tag{3}$$

where E represents the space of edges in the graph, and x_i and x_j are the label values of pixels, respectively. For mass segmentation, these values can be 0 and 1.

Grady [9] shows that Random Walker problem is the solution to Dirichlet problem. In their formulation, it is proposed the use of LU factorization of the Laplacian to solve the linear system of equations. However, other methods can be applied to solve the linear system.

The Random Walker algorithm uses the concept of seed pixels: users initially label a set of pixels associated with different classes and, taking into account the gray levels of these seeds, the algorithm tries to label all the pixels of the image. The Random Walker algorithm receives as input the image to be segmented and the label matrix with the labels provided by the user. The label given by the user can be of two types: background label or object label, which corresponds to the regions outside and inside of the lesion. Initially, the pixels have no labels associated until the user determines the object and background labels of chosen pixels. Therefore, an initial knowledge and effort is required to perform the segmentation. Figure 1 shows each stage of RW segmentation.

Figure 1a shows an image of a mammography patch containing a lesion. Figure 1b shows the initial labeling performed by the user. Although the user may not know the exact contour, he must select the seeds correctly, choosing pixels representing non-lesion areas and pixels inside the lesion. This stage can be a challenging task for lesions with ill-defined edges. Finally, Figure 1c shows the final segmentation.

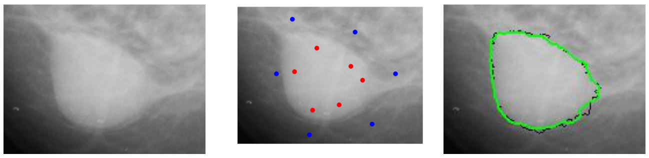

(a) (b) (c)

Figure 1: Random Walker Segmentation Process: (a) original image; (b) initial seeds; (c) segmented image.

In Random Walker, as in the majority of seed based techniques, the quality of segmentation depends directly on the positions of the initial seeds. Therefore, it depends on the user's knowledge to select seeds appropriately next to the edge of the object to be segmented. In case some seeds are initially labeled incorrectly, the algorithm may perform an undesired poor segmentation.

A. *Fuzzy Random Walker*

Our proposed approach is based on a modification in seeds initialization of the Random Walker algorithm, through the use of fuzzy logic. We named our proposed method as Fuzzy Random Walker (FRW). With our proposed modified Random Walker algorithm, we aim to reduce the need for initial specialist knowledge about the contour of the object of interest by reducing the effort in the selection of seeds.

Unlike classical RW, our proposal is based on the selection of seeds of only one class: the object of interest. We discard the selection of a background class because, from the seeds of the object of interest, we can estimate a frontier region separating object and background.

In the proposed approach, the initial localization of seeds is enough to estimate a fuzzy-gaussian function. Different from classical sets, elements of a fuzzy set have membership degrees to that set. The degree of membership to a fuzzy set indicates the certainty that the element belongs to that set [17]. A fuzzy element is defined as a fuzzy set, represented by a membership function $\mu_A : X \to [0, 1]$. Therefore, for all $x \in X$, μ_A indicates the certainty to which element x belongs to the fuzzy set.

In the proposed approach, the pixel will be labeled as background if the pertinence of a determined pixel to the background is higher than the pertinence of the same pixel to the object. Otherwise, the pixels remains unlabeled if it has not been previously selected by the user, or labeled as object, if previously selected. The membership function of associated to background and foreground are defined by Equation 4 and Equation 5:

$$\mu_{\text{Obj}}(i) = \exp\left(-\frac{(x_i - x_m)^2}{2\alpha_x s_x^2}\right) \exp\left(-\frac{(y_i - y_m)^2}{2\alpha_y s_y^2}\right), \tag{4}$$

$$\mu_{\text{Bkg}}(i) = 1 - \mu_{\text{Obj}}(i), \tag{5}$$

where $\mu_{\text{Bkg}}(i)$ is the fuzzy membership degree associated to the uncertainty of the i-th pixel belongs to the image background, whilst $\mu_{\text{Obj}}(i)$ is the fuzzy membership degree associated with the uncertainty of the i-th belongs to the object of interest. These fuzzy membership functions are Gaussian functions whose variables x_i and y_i correspond to the coordinates of the i-th pixel in the image, whereas x_m and y_m are the coordinates of the center of mass for the initially selected seeds; s_x and s_y are the standard deviation of initial points, whilst α_x and α_y are the weights of tuning of the Gaussian function, empirically determined according to the problem of interest. The s_x and s_y are obtained calculating the standard deviation of the position of the points selected by the user.

The label of each q-th pixel, l_q, is updated according to the following expression of Equation 6:

$$l_q = \begin{cases} l_{bkg}, & \mu_{\text{Bkg}}(q) > \mu_{\text{Obj}}(q) \\ l_q, & \mu_{\text{Bkg}}(q) \le \mu_{\text{Obj}}(q) \end{cases}, \tag{6}$$

where l_{bkg} represents the label of background. According to Equation 6, if $\mu_{\text{Bkg}}(q) \le \mu_{\text{Obj}}(q)$, the label continues with its initial labeling, i.e. undefined or object, if not selected or selected by the user, respectively.

The proposed initialization will be used as as entry to the RW algorithm. The flowchart of the proposed approach in shown in Figure 2:

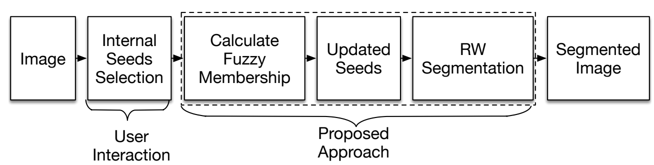

Figure 2: Flowchart of the Fuzzy Random Walker.

As shown in Figure 2, the proposed method starts with an image, or ROI, which is required that the user selects the internal seed points. For the process, we highlight that only the internal seeds are required. These seed points will be labeled as lesion. Next, the fuzzy membership is calculated based on those seeds selected by the user. Based on the fuzzy membership, the seeds are updated, where the background seed will be automatically defined. Next, the updated seeds will be used as entry to the RW algorithm, generating the final segmented image.

Figure 3 shows the each step of segmentation process of FRW. Figure 3a shows the original mammogram patch, which is submitted to initial labeling by the specialist. In the FRW, it is only necessary to select seeds inside the region, as shown in Figure 3b, reducing the effort compared to classical RW. Figure 3c shows the gaussian region estimated by the membership function. The extern area is considered as background, and the background labels are set automatically. The size of the area can be adjusted through the α parameter of Equation 5. After the labeling has been initialized, the segmentation starts. Figure 3d shows the result of segmentation, in green, compared to the ground truth, in black.

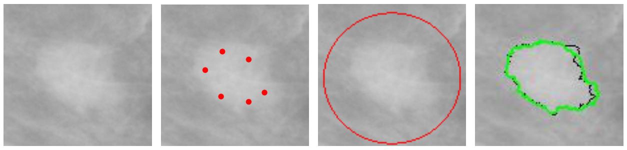

(a) (b) (c) (d)

Figure 3: Stages of the Fuzzy Random Walker. (a) Original Image; (b) Seeds Selection; (c) Fuzzy Gaussian Membership; (d) Segmented image.

IV. Methodology

A. Experimental Environment

In this work we use the Mini-MIAS public database [18] to perform the evaluations. Mini-MIAS was digitized at 50-micron pixel edge and has been reduced to 200-micron pixel edge and clipped so that every image is 1024 1024 pixels. The database consists of 322 mammography images from mediolateral oblique view, obtained from 161 patients. However, only 57 of those images contain lesions. The other images of the database are classified as normal, i.e. without lesion, or containing calcifications or asymmetry.

The ground truth image was obtained by a built supervised auxiliary software, based on an adaptive threshold, which uses the indications provided from database. Among the selected images, the masses contain different classes of abnormality: circumscribed, spiculated and ill-defined. Regions of interest were manually selected to perform the segmentation of the proposed technique.

To run the classical Random Walker algorithm, we used the python implementation, available at scikit-image library [19].

B. Metrics

The evaluation of results is based on the following metrics: sensitivity, specificity, Jaccard index, dice and balanced accuracy.

The chosen methods are defined based on True Positive (TP), False Positive (FP), True Negative (TN) and False Negative (FN). True positive and false positive rates measure the number of pixels correctly and incorrectly classified as lesion, respectively. True Negative and False Negative rates measure the number of pixels correctly and incorrectly classified as background, respectively.

Sensitivity (SE) evaluates the rate of pixels correctly as classified as lesion. Let GT be the ground truth, and S be the segmentation resulted from the segmentation algorithm, SE metric is defined by Equation 7:

$$\mathrm{SE} = \frac{\mathrm{TN}}{\mathrm{FP} + \mathrm{TN}}. \tag{7}$$

Specificity (SP) measures the rate of pixels correctly classified as background and is defined by Equation 8:

$$\mathrm{SP} = \frac{\mathrm{TP}}{\mathrm{TP} + \mathrm{FN}}, \tag{8}$$

Balanced accuracy (BAC) estimates the average of specificity and sensibility, and is defined by Equation 9:

$$\mathrm{BAC} = \frac{\mathrm{SP} + \mathrm{SE}}{2} \tag{9}$$

Jaccard index (J) indicates how similar the segmentation is when compared to its ground truth. The measure is given by the Equation 10:

$$\mathrm{J} = \frac{\mathrm{TP}}{\mathrm{TP} + \mathrm{FN} + \mathrm{FP}} \tag{10}$$

Dice is another metric commonly used for evaluation of segmentation algorithms and is defined by Equation 11:

$$\mathrm{Dice} = \frac{2 * TP}{S + GT} \tag{11}$$

V. Results

This section shows the segmentation results of Fuzzy Random Walks compared with its classical implementation, used by Wang and Landay [20]. The first analysis was done aiming to find the best parameter of classical Random Walker. The algorithm requires three parameters to be optimized: *sigma*, *mode*, and *tol*. The *sigma* value regulates the penalization coefficient for the random walker motion. The greater sigma, the more difficult the diffusion. Mode parameter indicates the mode for solving the linear system of equations in the Random Walker algorithm. We used three configurations for this parameter: brute force (bf), conjugate gradient (cg) and conjugate gradient with multigrid preconditioner (cg_mg). When using *bf*, the LU factorization of the Laplacian is computed. When using *cg*, the linear system is solved iteratively using the Conjugate Gradient method, and using cg_{mg}, a preconditioner is computed using a multigrid solver, then the solution is computed with the Conjugate Gradient. At last, the *tol* parameter sets the tolerance to achieve when solving the linear system of Random Walker. The tolerance value is applied only when solving the linear system using *cg* and cg_{mg} modes. Table I shows the parameter values used in this analysis:

Table I: Random Walker Parameter Exploration Space

Parameter	Values
Beta	5000, 10000, 20000, 30000, 40000
Mode	bf, cg, cg_mg
Tol	0.001, 0.05, 0.1, 0.2

Results from parameters tuning showed that Random Walker is very sensitive to correct selection of parameters. The default parameters provided by scikit-image library was not enough to perform an accurate segmentation to segment masses in mammography images. However, testing the parameters described in Table I we could obtain competitive segmentation results. The best configuration found for RW was obtained using parameters values of $sigma = 10000$, $mode = cg$ and $tol = 0.02$.

In the proposed approach, there is the addition of β parameter, which adjusts the size of gaussian region. We varied with the vales of 0.5, 1, 2, and 3. The best configuration of the proposed approach was obtained using the the following parameters: $beta = 1$, $sigma = 30000$, $mode = bf$. For bf mode there is no tolerance parameter. Results of segmentation from images of the database are shown in Figure 4. We used the images mdb010, mdb021, mdb028, mdb190, mdb132 and mdb312 as sample results of the database.

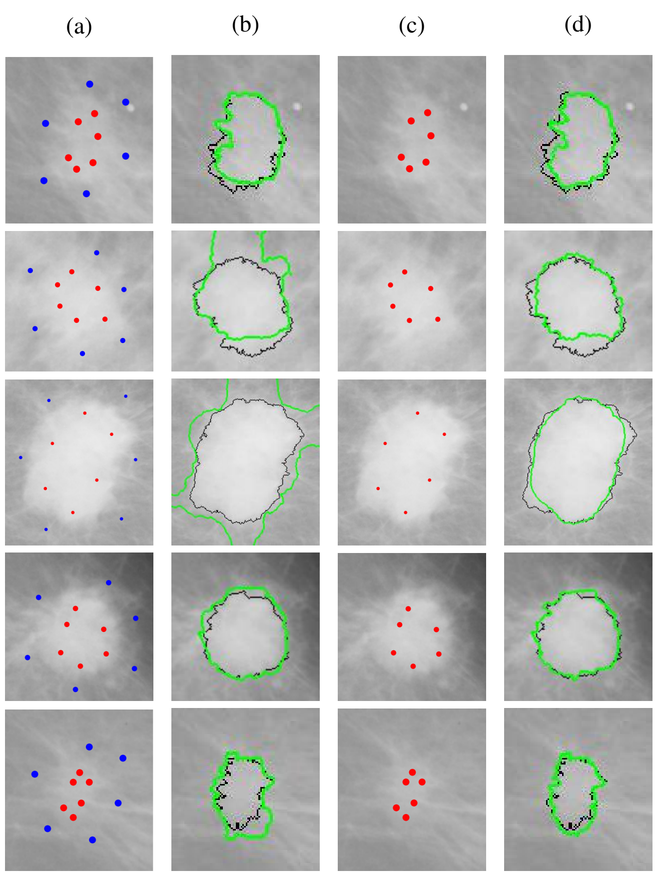

Figure 4: Comparison of segmentation of RW and FRW for the images mdb010, mdb021, mdb028, mdb190, mdb132 e mdb312. Column (a): RW seeds. Column (b): RW segmentation. Column (c): FRW seeds. Column (d) FRW segmentation.

In Figure 4, column (a) shows the seed points used for RW segmentation. The points in blue are the seeds labeled as background and the points in red are labeled as lesion. Column (b) show the segmentation obtained using the seeds points from column (a). The black contour represents the ground truth, while the green contour represents the segmentation of the algorithm. As can be observed, for same images, the RW algorithm does not perform well, missing some areas of the edges. Column (c) in Figure 4 shows the seeds used for the FRW. It is important to note that the internal seeds are at the same location used with classical RW. But no external seeds are necessary to perform the segmentation. The impact of this is the reduction of specialist effort and knowledge necessary to the problem. Finally, column (d) shows the segmentation obtained using the proposed approach. For the images in Figure 4, we can see that even without providing background seeds, the FRW was able to perform a segmentation close to the ground truth, with better results for the images that the RW had difficulties to segment.

We analyzed the ROC curve of different configurations using RW and the proposed approach. Figure 5 shows the behavior of configuration parameters of each technique. Results of Figure 5 show in green and blue the different configurations of RW and the proposed approach, respectively. The proposed approach have more configurations because it has one additional parameter compared to RW. That provides a positive aspect, giving more options to the user to select a configuration with higher true positive or lower false positive rate. On the other hand, the configuration processing can be more challenging. However, as can be seen in Figure 5, the configurations of the proposed method outperforms the classical RW when considering true positive and false positive rates. Moreover, the FRW has the advantage in the seed selection, being required only internal seeds labeling.

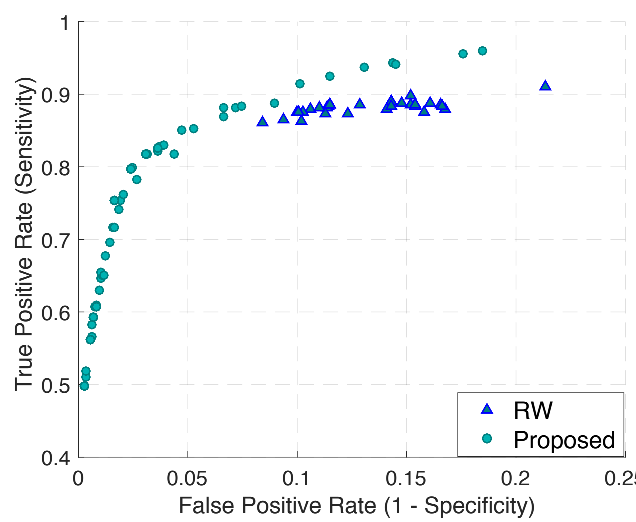

Figure 5: ROC Curve varying parameters of classical RW and the proposed approach.

To evaluate all the metrics, we chose the configurations with better values of Jaccard index and Dice, which are the configurations described previoulsy. With those settings selected, we analyzed all the metrics together and calculated the average of results, for all images. The results for the metrics are shown in Figure 6.

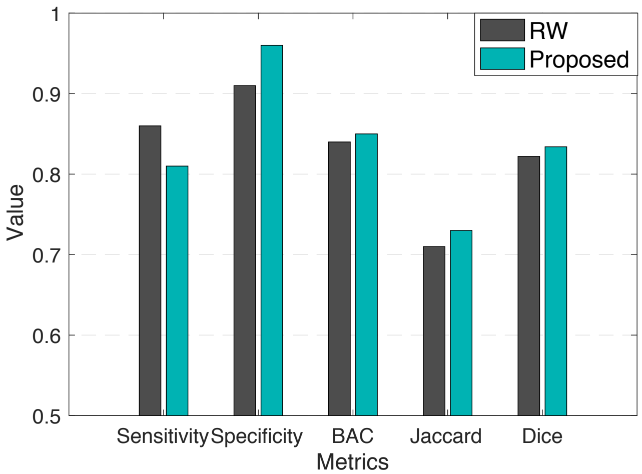

Figure 6: Comparison of Random Walker and the proposed approach, for the metrics of sensitivity, specificity, bac, jaccard index and dice.

Results from Figure 6 demonstrates that the proposed approach obtained better results for most of the metrics, compared with classical RW. Although RW obtained the higher value of sensitivity, the proposed method achieved the higher value for BAC, which measures the tradeoff between sensitivity and specificity. Furthermore, as can be seen in Figure 5, the sensitivity can be increased changing the configuration.

VI. Conclusion

This work proposed a new segmentation method based on Random Walker algorithm, applied to segmentation of masses in mammography images The proposed method, named Fuzzy Random Walker, uses a gaussian membership function to update the initial labeling. The evaluation was performed using 57 images from Mini-MIAS database, compared to the metrics of sensitivity, specificity, balanced accuracy, dice and Jaccard index.

Results showed that the proposed approach required less effort from the user, once the selection of background seed points is not necessary, as compared to traditional RW. As a drawback, the proposed method has the addition of a parameter that controls gaussian region.

When compared to Random Walks, the proposed approach obtained higher values for Balanced accuracy, Jaccard index, and dice. The proposed method also showed more interesting candidate solutions when considering true positive and false positive rate.

Finally, we could increase the performance of RW to segment masses in mammography images, while reducing the effort necessary in the initial stage. Future works aim to turn the process automatic and expand the dataset.

References

[1] World Health Organization, "WHO Position Paper on Mammography Screening," pp. 7–10, 2014.

[2] S. K. Bandyopadhyay, I. K. Maitra, and T. H. Kim, "Identification of abnormal masses in digital mammography images," *Proceedings - 2011 International Conference on Ubiquitous Computing and Multimedia Applications, UCMA 2011*, no. July 2015, pp. 35–41, 2012.

[3] D. C. Allred, J. M. Harvey, M. Berardo, and G. M. Clark, "Prognostic and predictive factors in breast cancer by immunohistochemical analysis." *Modern pathology : an official journal of the United States and Canadian Academy of Pathology, Inc*, vol. 11, no. 2, pp. 155–168, 1998.

[4] S. Litière, G. Werutsky, I. S. Fentiman, E. Rutgers, M. R. Christiaens, E. Van Limbergen, M. H. A. Baaijens, J. Bogaerts, and H. Bartelink, "Breast conserving therapy versus mastectomy for stage I-II breast cancer: 20 year follow-up of the EORTC 10801 phase 3 randomised trial," *The Lancet Oncology*, vol. 13, no. 4, pp. 412–419, 2012.

[5] W. I. Suleiman, S. J. Lewis, D. Georgian-Smith, M. G. Evanoff, and M. F. McEntee, "Number of mammography cases read per year is a strong predictor of sensitivity," *Journal of Medical Imaging*, vol. 1, no. 1, pp. 155–183, 2014.

[6] D. X. Wang, F. Yuan, and H. Sheng, "An algorithm for medical imaging identification based on edge detection and seed filling," in *ICCASM 2010 - 2010 International Conference on Computer Application and System Modeling, Proceedings*, vol. 15, 2010, pp. 547–548.

[7] S. Y. S. Ye, S. Z. S. Zheng, and W. H. W. Hao, "Medical image edge detection method based on adaptive facet model," *Computer Application and System Modeling (ICCASM), 2010 International Conference on*, vol. 3, pp. 574–578, 2010.

[8] V. Raman, P. Sumari, H. Then, and S. A. K. Al-Omari, "Review on Mammogram Mass Detection by Machine Learning Techniques," *International Journal of Computer and Electrical Engineering*, vol. 3, no. 6, pp. 873–879, 2011.

[9] L. Grady, "Random walks for image segmentation," *IEEE transactions on pattern analysis and machine intelligence*, vol. 28, no. 11, pp. 1768–1783, 2006.

[10] S.-w. Zheng, J. Liu, and C.-C. Liu, "A Random-Walk Based Breast Tumors Segmentation Algorithm for Mammograms," vol. 2, no. 2, pp. 66–74, 2013.

[11] S. Lewis and A. Dong, "Detection of breast tumor candidates using marker-controlled watershed segmentation and morphological analysis," in *Image Analysis and Interpretation (SSIAI), 2012 IEEE Southwest Symposium on*, April 2012, pp. 1–4.

[12] M. Eltoukhy and I. Faye, "An adaptive threshold method for mass detection in mammographic images," in *Signal and Image Processing Applications (ICSIPA), 2013 IEEE International Conference on*, Oct 2013, pp. 374–378.

[13] B. W. Hong and B. S. Sohn, "Segmentation of regions of interest in mammograms in a topographic approach," in *IEEE Transactions on Information Technology in Biomedicine*, vol. 14, no. 1. IEEE, 2010, pp. 129–139.

[14] F. R. Cordeiro, W. P. Santos, and A. G. Silva-Filhoa, "Segmentation of mammography by applying growcut for mass detection," in *Studies in Health Technology and Informatics*, vol. 192, no. 1-2, 2013, pp. 87–91.

[15] F. R. Cordeiro, W. P. Santos, and A. G. Silva-Filho, "A semi-supervised fuzzy growcut algorithm to segment and classify regions of interest of mammographic images," *Expert Systems with Applications*, vol. 65, pp. 116–126, 2016.

[16] L. Grady and G. Funka-Lea, "Multi-label image segmentation for medical applications based on graph-theoretic electrical potentials," in *Computer Vision and Mathematical Methods in Medical and Biomedical Image Analysis*. Springer, 2004, pp. 230–245.

[17] D. J. Dubois, H. Prade, and R. R. Yager, *Readings in fuzzy sets for intelligent systems*. Morgan Kaufmann, 2014.

[18] J. Suckling, J. Parker, D. Dance, S. Astley, I. Hutt, C. Boggis, I. Ricketts, E. Stamatakis, N. Cerneaz, S. Kok *et al.*, "The mammographic image analysis society digital mammogram database," in *Exerpta Medica. International Congress Series*, vol. 1069, 1994, pp. 375–378.

[19] S. Van der Walt, J. L. Schönberger, J. Nunez-Iglesias, F. Boulogne, J. D. Warner, N. Yager, E. Gouillart, and T. Yu, "scikit-image: image processing in python," *PeerJ*, vol. 2, p. e453, 2014.

[20] F. Wang and D. P. Landau, "Efficient, multiple-range random walk algorithm to calculate the eensity of states," *Physical Review Letters*, vol. 86, no. 10, p. 2050, 2001.